Motor Imagery for Brain-Computer Interfaces: A Review

Jingwei Luo

***Abstract*—Electroencephalogram-based motor imagery (MI) classification is an important paradigm of non-invasive brain-computer interface (BCI). Among various BCI paradigms, MI has gained significant attention due to its non-invasive nature and potential applications in assistive technology, rehabilitation, and human-computer interaction. This paper provides a comprehensive review of the motor imagery paradigm in BCIs, focusing on its principles, methodologies, and practical applications. We begin by discussing the neural basis of motor imagery and the typical EEG patterns associated with it, such as event-related desynchronization (ERD) and synchronization (ERS). The review then delves into the different experimental setups and signal processing techniques used to detect and classify motor imagery signals, including spatial filtering, feature extraction, and machine learning algorithms. We also examine the challenges and limitations of current MI-based BCIs, such as individual variability, signal noise, and user training requirements. Furthermore, we highlight recent advancements in the field, including hybrid BCI systems, real-time feedback mechanisms, and novel applications in neurorehabilitation and assistive devices. Finally, we discuss future directions and potential research avenues that could enhance the robustness and usability of motor imagery-based BCIs, making them more accessible and effective for a wide range of users.**

***Index Terms*—Brain-computer interface, motor imagery**

I. A BRIEF REVIEW OF EEG-BASED BCI SYSTEMS [1]

A brain-computer interface (BCI) establishes a direct communication pathway that enables the human brain to interact with external devices [2]. Electroencephalogram (EEG), which records the electrical activities on the scalp of the brain, is the most widely used input signal in non-invasive BCIs due to its affordability and convenience [3].

A closed-loop EEG-based BCI system, shown in Fig. 1, consists of the following components [1]:

1) *Signal acquisition* [4], which uses an EEG device to collect EEG signals from the scalp. In the early days, EEG devices used wired connections and gel to increase conductivity. Currently, wireless connections and dry electrodes are becoming increasingly popular.
2) *Signal processing* [5], which usually includes temporal filtering and spatial filtering. The former typically uses a bandpass filter to reduce interference and noise, such as muscle artifacts, eye blinks, and DC drift. The latter combines different EEG channels to increase the signal-to-noise ratio. Popular spatial filters include common spatial patterns (CSPs) [6], independent component analysis (ICA) [7], blind source separation [8], xDAWN [9], etc.
3) *Feature extraction*, for which time domain, frequency domain [10], time-frequency domain, Riemannian space [11], and/or functional brain connectivity [12] features could be used.
4) *Pattern recognition*, where depending on the application, a classifier or regression model is used.
5) *Controller*, which outputs a command to control an external device, e.g., a wheelchair or a drone, or to alter the behavior of an environment, e.g., the difficulty level of a video game. A controller may not be needed in certain applications, e.g., BCI spellers.

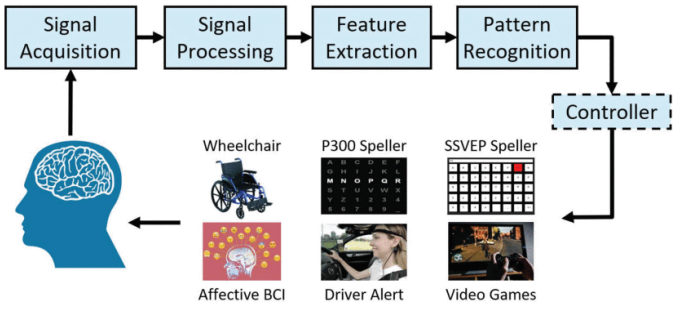

Fig. 1. Flowchart of a closed-loop EEG-based BCI system.

II. NEUROPHYSIOLOGICAL BASIS OF MOTOR IMAGERY [13], [14]

Motor imagery can be seen as mental rehearsal of a motor act without any overt motor output. This type of phenomenal experience imply that the subject feels himself performing a given action. It corresponds to the so-called internal imagery (or first person perspective) of sport psychologists [15]. Motor imagery may be experienced in two ways, or perspectives. The first person perspective which is supposed to rely on motor-kinesthetic information processing, and the third person perspective which would rely more on visuospatial processing. To my knowledge, no neurophysiological or neuroimaging studies concerned with this distinction has been reported. However, a few experiments in cognitive psychology have suggested the relevance to consider the distinction between visual and kinesthetic imagery [16].

Converging evidence from several sources indicates that mental imagination of movements involves similar brain regions/functions which are involved in programming and

J. Luo is with the School of Artificial Intelligence and Automation, Huazhong University of Science and Technology, Wuhan, China. Email: d202481524@hust.edu.cn.

preparing such movements [17]. According to this view, the main difference between performance and imagery is that in the latter case execution would be blocked at some cortico-spinal level [18].

Functional brain imaging studies monitoring changes in regional cerebral blood flow (rCBF) revealed indeed similar patterns of activity during motor imagery and actual movement performance. An increase of the rCBF has mainly been located in the supplementary motor area during imagination of sequential finger movements [19]. Moreover, recent positron emission tomography (PET) [18] and functional magnetic resonance imaging (fMRI) studies [20] revealed activation of a number of cortical and subcortical areas, including, e.g., the premotor cortex, the anterior cingulate gyrus, superior and inferior parietal areas, and the cerebellum. Thus, activation has been observed in various structures involved in the early stage of motor control (i.e., motor programming), but not in the primary sensorimotor cortex. More recent fMRI studies, in contrast, detected some activation in the primary motor cortex during motor imagery, though to a lesser extent than during actual motor performance [21]. Increased motor cortex activation during motor imagery has been supported by studies using transcranial magnetic stimulation in showing an increase of motor responses during mental imagination of movements [22].

Several EEG studies further confirm the notion that motor imagery can activate primary sensorimotor areas [23]. It induces changes in the sensory-motor rhythms (SMR) of corresponding areas of the cerebral cortex, which primarily involve modulations of the μ rhythm (8-12 Hz) and the β rhythm (14-30 Hz) [17]. Specifically, when an MI starts, these rhythmic activities decrease, resulting in event-related desynchronization (ERD); at the end of an MI, these rhythmic activities increase, resulting in event-related synchronization (ERS) [24].

A blocking of the central mu rhythm with motor imagery was reported in early clinical EEG observations [25]. Similar cortical activity over the contralateral hand area during execution and imagination of hand movement has further been found with dc potential measurements [23] and based on dipole source analysis of electric and magnetic fields [26]. Furthermore, high-resolution EEG experiments [27] showed that independent of the required motor task, imagination versus overt execution of a given movement, the most prominent EEG changes were localized over the corresponding primary sensorimotor cortex. During the imagination of a right-hand or left-hand movement, for example, a similar event-related desynchronization (ERD) over the contralateral hand area as is usually found during planning or preparation of a real movement is found. This imagination-related ERD shows different time courses in the alpha and beta bands (Fig. 2, upper panel). Similar to the self-paced movement task, the ERD in the beta band shows a fast recovery and is followed by a short-lasting event-related synchronization (ERS). Examples for the localization of beta ERS mapped on the reconstructed cortical surface of one representative subject (Fig. 2, lower panel) illustrate a focus close to the primary hand area after both a real executed and an imagined right-hand movement. This observation is in line with recent neuromagnetic studies suggesting that the central 20-Hz activity mainly originates in the primary sensorimotor cortex [28] and, moreover, documents the supposed similarity of neural circuitry involved in mental representation and movement execution.

It is of interest, that during overt execution of the movement, the initially contralateral ERD develops a bilateral distribution [29], whereas during mental simulation this ERD remains mostly limited to the contralateral hemisphere. This means that the suppression of mu and central beta rhythms is more pronounced at the contralateral hemisphere when subjects imagine one-sided hand movements [27] than when they actually perform such movements. This observation led us to utilize motor imagery as control strategy to achieve asymmetrical electrocortical responses and to use, e.g., left-right differences in the sensorimotor EEG to provide a control option in one dimension [30]. Besides this, MI also applies to different parts of the body such as the movement of the left hand, right hand, tongue [31], left foot, right foot movement [32], wrist movement (flexion, extension, pronation, and supination) [33], elbow flexion/extension, forearm pronation/supination, hand open/close [34], and finger movements [35].

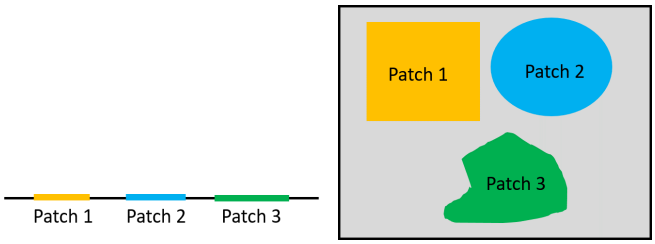

(a) (b)

Fig. 2. Patches in 1D and 2D input domains.

TABLE I
TYPES OF BRAIN WAVES.

Type of waves	Frequency band (Hz)	MI-related frequency bands (Hz)	Amplitude (μv)	Lobe of brain	Available in
Delta	1-3	-	20-200	Cortex/Thalamus	It appears when we are energetic after waking up.
Theta	4-7	-	10	Hippocampal	It occurs when we are disappointed.
Alpha	8-13	8-12	2-100	Parietal occipital	It occurs when our mind is alert.
Beta	13-30	16-24	5-10	Frontal	It occurs in the most active state like in reasoning.
Gamma	30-100	30-35	-	Between frontal and parietal lobe	It occurs when we combine different senses like sound and sight.

III. Experimental Paradigm

[13]

To effectively decode EEG signals of MI, BCI research typically employs a variety of experimental setups designed to simulate and record the MI process. Below is a typical setup for an MI-based BCI experiment.

In the standard paradigm, the experimental task is to imagine either right-hand or left-hand movement depending on a visually presented cue stimulus. The subject fixates on a computer monitor 150 cm in front of her/him. Each trial is 8s long and starts with the presentation of a fixation cross at the center of the monitor, followed by a short warning tone (beep) at 2000 ms. At 3000 ms, the fixation cross is overlaid with an arrow at the center of the monitor for 1250 ms, pointing either to the left or to the right (Fig. 3, upper part). Depending on the direction of the arrow, the subject is instructed to imagine, e.g., a movement of the left or the right hand.

Two different types of feedback are used: 1. discrete delayed feedback and 2. continuous feedback. Discrete feedback consists of a symbol presented in the center of the monitor at 6000 ms: the type of symbol (large or small "+" or "-" or "0") depends on how well a subject-specific classifier can distinguish the two EEG patterns related to left versus right motor imagery in a fixed time window from 3250 to 4250 ms. In the case of continuous feedback, the imagination task is controlled by means of a horizontal feedback bar. Depending on the cue stimulus, the subject's task is to extent a bar toward the right or left boundary of the monitor by mental imagination of moving the right or left hand, respectively. The bar appears at time 4250 ms and is presented over a 4-s period (Fig. 3, lower part). The length of the bar directly corresponds to the linear distance function obtained by online analysis of the EEG signals [30]. Normally, each session consists of four experimental runs of 40 trials (20 "left" and 20 "right" trials) and lasts for about 1 h. The sequence of "left" and "right" trials, as well as the duration of the breaks between consecutive trials (ranging between 500 and 2500 ms), is randomized throughout each experimental run.

IV. Data Acquisition

A. EEG recordings

[36]

EEG captures physiological activities of the body by recording electrical signals which are the produced postsynaptic potentials by cortical neurons [37]. The electrical signals are recorded via conducting electrodes that are placed on the scalp according to the well-known 10-20 international placement system as stated in Fig. 3, motor imagery related electrodes are identified in blue color [38]. Each electrode records a one-dimensional vector of raw EEG data. The signals are obtained on the three-dimensional scalp surface through volume conduction across multiple brain tissue [37]. Hence, EEG signals are prone to artifacts originating from different parts of the body like the eye, head, neck, or any other muscle. Moreover, the power cable of the recording device and electrode displacement might both cause some artifacts. This form of recording EEG produces weak, non-stationary, and low signal-to-noise ratio signals. Consequently, it complicates the classification and interpretation of signals belonging to a particular case of consideration.

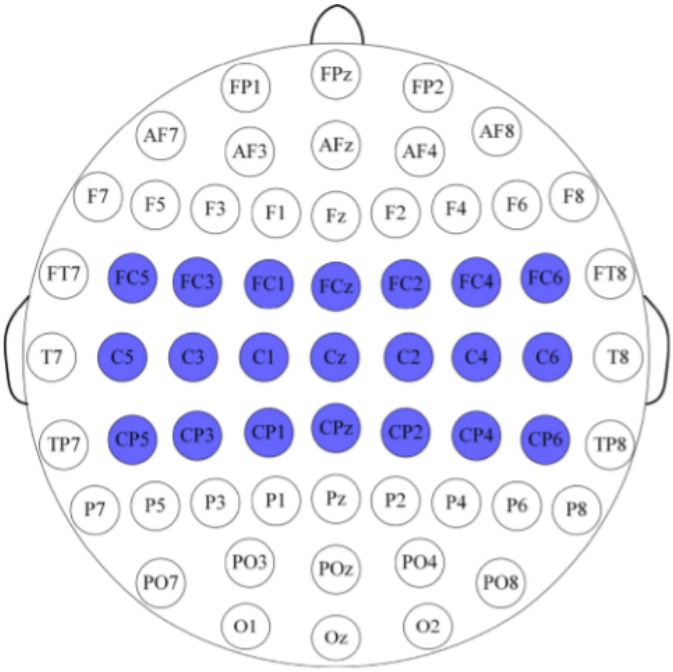

Fig. 3. EEG electrodes placement according to the 10-20 system. The related motor imagery electrodes are identified in blue color.

Despite the inherent drawbacks in raw EEG, it has some advantages over other neurological imaging techniques. It characterized by low cost, portability, and causes no side effects because of its non-invasive style [31]. Thus, EEG has a variety of applications whether as a screening method or for hypothesis-based diagnostics. Depending on the shape of waves, e.g. rapid spikes waves or slow waves, several forms of brain disorders can be assessed, such as epilepsy [39], tumors [39], Alzheimer [40], sleep disorder [41], etc.

Basically, the amplitude and frequency values in EEG signals are used for discriminating various physiological activities. The amplitude is normally fluctuating in microvolts. The frequency range in EEG signals can be split into several bands as shown in Table I [42]. The most popular motor imagery frequency bands are also stated in the table. It should be noted that when the Alpha band is recorded from the sensorimotor cortex then it is called mu band. The Gamma band can be recorded consistently using internal electrodes in order to better capture it as it is being weak at the scalp [43]. Slightly different frequency bands or ranges may be found in the literature.

EEG signals are complex in their nature and there exists acute dependency of signal quality on the mental state of the user. Studies proved that the classification accuracy of an intelligent system for a certain task was better at the beginning of the trial than the accuracy at the end of that trial [43]. Therefore, recording or selecting an EEG dataset is crucial for training, validating, and testing machine learning models.

B. Acquisition Process

[44]

1) *Preparation*. Ambient electrical noise can significantly interfere with EEG recordings. When setting up a laboratory, and periodically throughout the course of data collection, it is advisable to check noise levels using a handheld gauss meter sensitive to the electrical noise frequency range emitted by power lines, computers, and other electrical appliances. In China, this frequency range is typically 50 Hz, while in the USA, it can be 60 Hz.
   Ensure that the laboratory environment is quiet and free from electromagnetic interference. One effective method for reducing the influence of electrical noise is to collect EEG data in an electrically shielded room or chamber. If such a facility is not available, and a gauss meter indicates the presence of electrical noise, relocating the offending equipment a short distance away from the electrodes and electrode wires can often mitigate the impact of noise on recordings.
   When the study participant arrives at the lab, make them feel comfortable, explain the experiment in detail, and ensure they understand all aspects of it. Have the subject sign the consent form and adjust the stimulation setup to their comfort (e.g., chair height, screen distance, or sound levels) to minimize movement and muscle tension, thereby avoiding interference with the EEG signals.
2) *Adjusting the Equipment*. Select the correct cap size by measuring the participant's head circumference in centimeters (hat size) around the widest point on the head using a flexible tape measure. Cap sizes typically range from 52 to 60 cm in increments of 2 cm. Most labs have 54, 56, 58, and 60 cm sizes as part of a standard EEG setup. If the measurement falls between sizes, try the next larger size. The cap should fit snugly. Ensuring a proper fit is crucial, as a cap that is too large may reduce the quality of EEG recordings or make electrode preparation and impedance reduction more challenging. To check the fit, ask the participant to nod their head up and down and turn it side to side. If the cap shifts, it is too big, and a smaller size should be used. Additionally, when the cap is on the participant's head, gently press down on one of the electrode adaptors towards the scalp. If the adaptor bounces back, there may be too much space between the adaptor and the scalp, indicating that a smaller cap size should be tried. Once the correct cap size is determined, remove the cap from the head and snap in the electrodes.
   Plug the electrodes into the EEG amplifier at the appropriate locations. Consult the EEG acquisition software materials for instructions on how to designate channels. Depending on the setup and equipment, it may be necessary to label the channels on the amplifier (e.g., Ground, FP1, CZ, REOG, LEOG).
   Before placing the cap on the participant's head, roughly measure the distance between the participant's nasion (bridge of the nose) and inion (bump on the lower base of the skull: to find the inion, place your hand in the middle of the neck and slide upwards) using your hands. The FPz electrode should be placed about 10% of this distance above the nasion in the middle of the forehead. Place the front of the cap on the participant's forehead with FPz in this position, ask the participant to hold the cap in place, and then pull the cap over the head. Next, adjust the position of the CZ electrode so it lies halfway between the nasion and the inion.
   Minimize the impedance of the electrical connection between the electrode and the scalp by applying abrasive electrolyte gel. Specifically, fill syringes with abrasive electrolyte gel, and then fill the electrodes with gel using those syringes (ensure the plastic tip of the syringe touches the scalp). Gently scrub the scalp through the electrode opening by twirling the cotton end of the cotton swab between your thumb and index finger.
3) *Begin Data Collection*. Open the EEG acquisition software and load the experiment file. Observe the resting activity of all the electrodes, and ensure there are no "bad" channels; that is, electrodes that produce flat line signals or show excessive activity while the participant is resting. If any bad channels are suspected, it may be necessary to apply more electrode gel and scrub to minimize impedance or replace the electrode. Instruct the participant to avoid blinking and tensing muscles in their forehead or jaw, as these actions can introduce noise into the EEG data.
   Once all the electrode signals appear acceptable, begin recording and start the experiment file. If collecting data for an MI experiment or other design where the timing of stimulus presentation is crucial for signal processing, carefully observe the first few trials to ensure that the stimulus presentation software is sending "trigger" markers for stimulus presentation. If timing markers are not being sent, the data cannot be processed using stimulus presentation as a reference point, which is essential for MI designs.

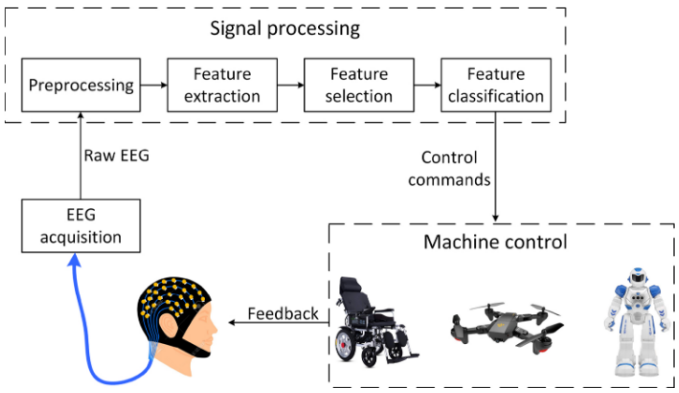

Fig. 4. A block diagram for the general BCI system.

V. Signal Processing

[36]

A. Preprocessing of raw data

Raw EEG signals usually contain plenty of undesirable background noise that requires elimination before beginning the real analysis. Also, sometimes it is desirable to enhance the raw EEG to better fit the requirements. For those reasons, one or more of the listed below preprocessing methods [45]–[48] might be applied.

- Notch filtering to remove power line noise at 50 Hz or 60 Hz.
- High-pass filtering with a low cutoff frequency to remove baseline drift.
- Band-pass filtering to select the desirable band(s).
- Clipping the amplitude of EEG signals either by forcing it to be within a specific range or based on the mean and the standard deviation.
- Canceling several samples from the beginning and/or from the end of the signal to remove possible acute artifacts.
- Normalizing the data to zero mean and unit variance using z-score. This can speed up the convergence and avoid trapping by local minima.
- Downsampling the signal for speeding up the computation and reducing memory storage.
- Selection of specific electrodes based on the goal of the application.
- Interpolating of corrupted signals.
- Artifact rejection such as the electrooculogram (EOG) and the electromyogram (EMG) artifacts. This can be achieved in different ways such as a thresholding-based method or data-driven method like the Independent Component Analysis (ICA).
- Referencing using either an electrode (Cz and Fz are often employed as reference electrodes) or the average of signals from all electrodes. Common average referencing (CAR) and Laplacian are widely used spatial filters. Referencing helps to eliminate some of the background noise.

B. Processing features

The processed EEG data go through feature extraction, feature selection, and feature classification phases in order to achieve a decision after that. According to [42], the types of usually used EEG features in BCI systems can be grouped into manually selected, statistical, and data-driven adaptive features. Those three phases intensively employed numerous traditional signal processing approaches. Table II summarizes the most widely used signal processing approaches for dealing with features in EEG applications. Based on the fact that EEG signals are dynamic and highly complex [49], selecting a set of tools for dealing with features would be crucial.

Feature extraction can be achieved based on time, frequency, and/or spatial information contained in the signals. Extracting features depending only on temporal information discards spectral information, likewise, if features are extracted based on only spectral information then the temporal information will be discarded. Hence, either of these techniques is considered weak in extracting salient features. Timefrequency approaches are more vigorous since they relate temporal information with spectral information into each single extracted feature [49]. It must be kept in mind the differences among the time-frequency approaches. For example, STFT is considered a static method in terms of time and frequency resolution because of the fixed-length window used along with the signal analysis; while wavelet transform delivers dynamic features due to the used multiresolution window [50]. Relying on time-frequency approaches is beneficial in the analysis because of the nonstationary nature of EEG signals. Spatial domain approaches can be combined with time and/or frequency domain approaches aiming at increasing the classification accuracy.

TABLE II
A SUMMERY LIST OF SIGNAL PROCESSING TECHNIQUES FOR FEATURES EXTRACTION, SELECTION, AND CLASSIFICATION.

Feature extraction	Time-domain	Autoregressive (AR) Adaptive autoregressive Root-mean-square (RMS) Integreated EEG (IEEG)
	Frequency-domain	Fast Fourier transform (FFT) Welch's method Local characteristic-scale decomposition (LCD)
	Time-frequency domain	Short-time Fourier transform (STFT) Wavelet transform (WT) Discrete wavelet transform (DWT)
	Spatial domain	Common spatial pattern (CSP) Common spatio-spectral pattern (CSSP) Common sparse spatio-spectral patterns (CSSSP) Sub-band common spatial pattern (SBCSP)
Feature selection	Statistical transformation	Principal component analysis (PCA) Independent component analysis (ICA)
	Filter bank	Filter bank CSP (FBCSP) Discriminant filter bank CSP (DFBCSP) Sparse filter bank CSP (SFBCSP)
	Evolutionary algorithms (EAs)	Particle swarm optimization (PSO) Differential evolution (DE) Artificial bee colony (ABC) Ant colony optimization(ACO) Genetic algorithms (GAs)
Classification	Linear	Support-vector machines (SVMs) Linear discriminant analysis (LDA) Naive Bayes Logistic regression (LR)
	Nonlinear	Bayes quadratic Hidden Markov model (HMM)
	Nearest neighbor	k-nearest neighbor analysis (k-NN)
	Artificial neural network (ANN)	Multi-layer perceptron (MLP) Radial basis function (RBF) Deep neural network (DNN)

With the spatial domain approaches the most effective EEG channels can be identified [51] and used with higher weights than those less effective channels.

Normally, high dimensional feature sets are extracted from EEG data. For this, statistical transformation techniques such as PCA and ICA are used for dimensionality reduction and feature selection, however, these techniques are computationally demanding and they may decrease the classification accuracy [52]. Evolutionary algorithms (EAs) approaches involve optimization methods for selecting features from large sets of features, thus EAs could manage the high dimensionality problem [53]. The use of filter bank approaches such as CSP had a high impact on dealing with features in EEG data [43]. Neural network (NN) as a wealth approach uses a framework that combines all of the three phases extraction, selection, and classification into a single pipeline. Despite the lengthy training stage in NN, new unseen data can be analyzed as soon as the network parameters are fixed [42]. This results in more efficient computations which in turn permits using NN in online EEG analysis.

A large number of studies [54]–[58] used more than one approach in each of the three phases extraction, selection, and classification. Noteworthy, many BCI systems do not involve selection phase, however, those systems that involve a selection procedure seek for salient features to achieve higher accuracy.

ACKNOWLEDGEMENT

This research was supported by the National Natural Science Foundation of China Grant 61873321.

REFERENCES

[1] D. Wu, Y. Xu, and B.-L. Lu, "Transfer learning for eeg-based brain–computer interfaces: A review of progress made since 2016," *IEEE Transactions on Cognitive and Developmental Systems*, vol. 14, no. 1, pp. 4–19, 2020.

[2] B. Graimann, B. Allison, and G. Pfurtscheller, "Brain-computer interfaces: A gentle introduction," in *Brain-computer interfaces: Revolutionizing human-computer interaction*. Springer, 2010, pp. 1–27.

[3] L. F. Nicolas-Alonso and J. Gomez-Gil, "Brain computer interfaces, a review," *sensors*, vol. 12, no. 2, pp. 1211–1279, 2012.

[4] L.-D. Liao, C.-T. Lin, K. McDowell, A. Wickenden, K. Gramann, T.-P. Jung, L.-W. Ko, and J.-Y. Chang, "Biosensor technologies for augmented brain-computer interfaces in the next decades," *Proc. of the IEEE*, vol. 100, no. 2, pp. 1553–1566, 2012.

[5] S. Makeig, C. Kothe, T. Mullen, N. Bigdely-Shamlo, Z. Zhang, and K. Kreutz-Delgado, "Evolving signal processing for brain-computer interfaces," *Proc. of the IEEE*, vol. 100, no. Special Centennial Issue, pp. 1567–1584, 2012.

[6] H. Ramoser, J. Muller-Gerking, and G. Pfurtscheller, "Optimal spatial filtering of single trial eeg during imagined hand movement," *IEEE transactions on rehabilitation engineering*, vol. 8, no. 4, pp. 441–446, 2000.

[7] S. Makeig, A. J. Bell, T.-P. Jung, and T. J. Sejnowski, "Independent component analysis of electroencephalographic data," in *Advances in Neural Information Processing Systems*, Denver, CO, Dec. 1996, pp. 145–151.

[8] T.-P. Jung, S. Makeig, C. Humphries, T.-W. Lee, M. J. Mckeown, V. Iragui, and T. J. Sejnowski, "Removing electroencephalographic artifacts by blind source separation," *Psychophysiology*, vol. 37, no. 2, pp. 163–178, 2000.

[9] B. Rivet, A. Souloumiac, V. Attina, and G. Gibert, "xdawn algorithm to enhance evoked potentials: application to brain–computer interface," *IEEE Transactions on Biomedical Engineering*, vol. 56, no. 8, pp. 2035–2043, 2009.

[10] X.-W. Wang, D. Nie, and B.-L. Lu, "Emotional state classification from EEG data using machine learning approach," *Neurocomputing*, vol. 129, pp. 94–106, 2014.

[11] F. Yger, M. Berar, and F. Lotte, "Riemannian approaches in brain-computer interfaces: a review," *IEEE Trans. on Neural Systems and Rehabilitation Engineering*, vol. 25, no. 10, pp. 1753–1762, 2017.

[12] X. Wu, W.-L. Zheng, and B.-L. Lu, "Identifying functional brain connectivity patterns for EEG-based emotion recognition," in *Proc. 9th Int'l IEEE/EMBS Conf. on Neural Engineering*, San Francisco, CA, Mar. 2019, pp. 235–238.

[13] G. Pfurtscheller and C. Neuper, "Motor imagery and direct brain-computer communication," *Proceedings of the IEEE*, vol. 89, no. 7, pp. 1123–1134, 2001.

[14] J. Decety, "The neurophysiological basis of motor imagery," *Behavioural brain research*, vol. 77, no. 1-2, pp. 45–52, 1996.

[15] D. M. Landers, "The effects of mental practice on motor skill learning and performance: A meta-analysis." *Journal of sport psychology*, vol. 5, no. 1, pp. 25–57, 1983.

[16] M. Denis, "Visual imagery and the use of mental practice in the development of motor skills," *Canadian Journal of Applied Sport Sciences*, vol. 10, no. 4, pp. 45–165, 1985.

[17] M. Jeannerod, "Mental imagery in the motor context," *Neuropsychologia*, vol. 33, no. 11, pp. 1419–1432, 1995.

[18] J. Decety, D. Perani, M. Jeannerod, V. Bettinardi, B. Tadary, R. Woods, J. C. Mazziotta, and F. Fazio, "Mapping motor representations with positron emission tomography," *Nature*, vol. 371, no. 6498, pp. 600–602, 1994.

[19] P. E. Roland, B. Larsen, N. A. Lassen, and E. Skinhoj, "Supplementary motor area and other cortical areas in organization of voluntary movements in man," *Journal of neurophysiology*, vol. 43, no. 1, pp. 118–136, 1980.

[20] S. M. Rao, J. Binder, P. Bandettini, T. Hammeke, F. Yetkin, A. Jesmanowicz, L. Lisk, G. Morris, W. Mueller, L. Estkowski *et al.*, "Functional magnetic resonance imaging of complex human movements," *Neurology*, vol. 43, no. 11, pp. 2311–2311, 1993.

[21] M. Hallett, J. Fieldman, L. G. Cohen, N. Sadato, and A. Pascual-Leone, "Involvement of primary motor cortex in motor imagery and mental practice," *Behavioral and Brain Sciences*, vol. 17, no. 2, pp. 210–210, 1994.

[22] S. Gandevia and J. Rothwell, "Knowledge of motor commands and the recruitment of human motoneurons," *Brain*, vol. 110, no. 5, pp. 1117–1130, 1987.

[23] R. Beisteiner, P. Höllinger, G. Lindinger, W. Lang, and A. Berthoz, "Mental representations of movements. brain potentials associated with imagination of hand movements," *Electroencephalography and Clinical Neurophysiology/Evoked Potentials Section*, vol. 96, no. 2, pp. 183–193, 1995.

[24] G. Pfurtscheller, C. Neuper, D. Flotzinger, and M. Pregenzer, "Eeg-based discrimination between imagination of right and left hand movement," *Electroencephalography and clinical Neurophysiology*, vol. 103, no. 6, pp. 642–651, 1997.

[25] H. Gastaut, "'etude'electrocorticographique de la reactivite des rythmes rolandiques," *Rev. neurol.*, vol. 87, pp. 176–182, 1952.

[26] W. Lang, D. Cheyne, P. Höllinger, W. Gerschlager, and G. Lindinger, "Electric and magnetic fields of the brain accompanying internal simulation of movement," *Cognitive brain research*, vol. 3, no. 2, pp. 125–129, 1996.

[27] G. Pfurtscheller and C. Neuper, "Motor imagery activates primary sensorimotor area in humans," *Neuroscience letters*, vol. 239, no. 2-3, pp. 65–68, 1997.

[28] R. Salmelin, M. Hámáaláinen, M. Kajola, and R. Hari, "Functional segregation of movement-related rhythmic activity in the human brain," *Neuroimage*, vol. 2, no. 4, pp. 237–243, 1995.

[29] C. Toro, G. Deuschl, R. Thatcher, S. Sato, C. Kufta, and M. Hallett, "Event-related desynchronization and movement-related cortical potentials on the ecog and eeg," *Electroencephalography and Clinical Neurophysiology/Evoked Potentials Section*, vol. 93, no. 5, pp. 380–389, 1994.

[30] C. Neuper, A. Schlögl, and G. Pfurtscheller, "Enhancement of left-right sensorimotor eeg differences during feedback-regulated motor imagery," *Journal of Clinical Neurophysiology*, vol. 16, no. 4, pp. 373–382, 1999.

[31] W. Qiao and X. Bi, "Deep spatial-temporal neural network for classification of eeg-based motor imagery," in *Proceedings of the 2019 international conference on artificial intelligence and computer science*, 2019, pp. 265–272.

[32] M. Tariq, P. M. Trivailo, and M. Simic, "Mu-beta event-related (de) synchronization and eeg classification of left-right foot dorsiflexion

kinaesthetic motor imagery for bci," *Plos one*, vol. 15, no. 3, p. e0230184, 2020.
[33] X. Ma, S. Qiu, W. Wei, S. Wang, and H. He, "Deep channel-correlation network for motor imagery decoding from the same limb," *IEEE Transactions on Neural Systems and Rehabilitation Engineering*, vol. 28, no. 1, pp. 297–306, 2019.
[34] N. Mammone, C. Ieracitano, and F. C. Morabito, "A deep cnn approach to decode motor preparation of upper limbs from time–frequency maps of eeg signals at source level," *Neural Networks*, vol. 124, pp. 357–372, 2020.
[35] R. Alazrai, M. Abuhijleh, H. Alwanni, and M. I. Daoud, "A deep learning framework for decoding motor imagery tasks of the same hand using eeg signals," *IEEE Access*, vol. 7, pp. 109 612–109 627, 2019.
[36] A. Al-Saegh, S. A. Dawwd, and J. M. Abdul-Jabbar, "Deep learning for motor imagery eeg-based classification: A review," *Biomedical Signal Processing and Control*, vol. 63, p. 102172, 2021.
[37] M. Sazgar, M. G. Young, M. Sazgar, and M. G. Young, "Overview of eeg, electrode placement, and montages," *Absolute epilepsy and EEG rotation review: Essentials for trainees*, pp. 117–125, 2019.
[38] O. Kwon, M. Lee, C. Guan, and S. Lee, "Subject-independent brain-computer interfaces based on deep convolutional neural networks," *IEEE Trans. on Neural Networks and Learning Systems*, 2020, in press.
[39] W. Mardini, M. M. B. Yassein, R. Al-Rawashdeh, S. Aljawarneh, Y. Khamayseh, and O. Meqdadi, "Enhanced detection of epileptic seizure using eeg signals in combination with machine learning classifiers," *IEEE Access*, vol. 8, pp. 24 046–24 055, 2020.
[40] R. Pandya, S. Nadiadwala, R. Shah, and M. Shah, "Buildout of methodology for meticulous diagnosis of k-complex in eeg for aiding the detection of alzheimer's by artificial intelligence," *Augmented Human Research*, vol. 5, no. 3, pp. 1–8, 2020.
[41] D. Geng, D. Yang, M. Cai, and L. Zheng, "A novel microwave treatment for sleep disorders and classification of sleep stages using multi-scale entropy," *Entropy*, vol. 22, no. 3, p. 347, 2020.
[42] P. Wang, A. Jiang, X. Liu, J. Shang, and L. Zhang, "Lstm-based eeg classification in motor imagery tasks," *IEEE transactions on neural systems and rehabilitation engineering*, vol. 26, no. 11, pp. 2086–2095, 2018.
[43] N. Padfield, J. Zabalza, H. Zhao, V. Masero, and J. Ren, "Eeg-based brain-computer interfaces using motor-imagery: Techniques and challenges," *Sensors*, vol. 19, no. 6, p. 1423, 2019.
[44] G. A. Light, L. E. Williams, F. Minow, J. Sprock, A. Rissling, R. Sharp, N. R. Swerdlow, and D. L. Braff, "Electroencephalography (eeg) and event-related potentials (erps) with human participants," *Current protocols in neuroscience*, vol. 52, no. 1, pp. 6–25, 2010.
[45] Z. Tayeb, J. Fedjaev, N. Ghaboosi, C. Richter, L. Everding, X. Qu, Y. Wu, G. Cheng, and J. Conradt, "Validating deep neural networks for online decoding of motor imagery movements from eeg signals," *Sensors*, vol. 19, no. 1, p. 210, 2019.
[46] X. Tang, W. Li, X. Li, W. Ma, and X. Dang, "Motor imagery eeg recognition based on conditional optimization empirical mode decomposition and multi-scale convolutional neural network," *Expert Systems with Applications*, vol. 149, p. 113285, 2020.
[47] S. A. Ludwig and J. Kong, "Investigation of different classifiers and channel configurations of a mobile p300-based brain–computer interface," *Medical & biological engineering & computing*, vol. 55, pp. 2143–2154, 2017.
[48] T. K. Reddy, V. Arora, S. Kumar, L. Behera, Y.-K. Wang, and C.-T. Lin, "Electroencephalogram based reaction time prediction with differential phase synchrony representations using co-operative multi-task deep neural networks," *IEEE Transactions on Emerging Topics in Computational Intelligence*, vol. 3, no. 5, pp. 369–379, 2019.
[49] H. K. Lee and Y.-S. Choi, "Application of continuous wavelet transform and convolutional neural network in decoding motor imagery brain-computer interface," *Entropy*, vol. 21, no. 12, p. 1199, 2019.
[50] C. Herff, D. J. Krusienski, and P. Kubben, "The potential of stereotactic-eeg for brain-computer interfaces: current progress and future directions," *Frontiers in neuroscience*, vol. 14, p. 123, 2020.
[51] B. H. Yilmaz, C. M. Yilmaz, and C. Kose, "Diversity in a signal-to-image transformation approach for eeg-based motor imagery task classification," *Medical & biological engineering & computing*, vol. 58, pp. 443–459, 2020.
[52] N. Lu, T. Li, X. Ren, and H. Miao, "A deep learning scheme for motor imagery classification based on restricted boltzmann machines," *IEEE transactions on neural systems and rehabilitation engineering*, vol. 25, no. 6, pp. 566–576, 2016.
[53] P. Tan, X. Wang, and Y. Wang, "Dimensionality reduction in evolutionary algorithms-based feature selection for motor imagery brain-computer interface," *Swarm and Evolutionary Computation*, vol. 52, p. 100597, 2020.
[54] M. Z. Baig, N. Aslam, H. P. Shum, and L. Zhang, "Differential evolution algorithm as a tool for optimal feature subset selection in motor imagery eeg," *Expert Systems with Applications*, vol. 90, pp. 184–195, 2017.
[55] J. Kevric and A. Subasi, "Comparison of signal decomposition methods in classification of eeg signals for motor-imagery bci system," *Biomedical Signal Processing and Control*, vol. 31, pp. 398–406, 2017.
[56] M. Dai, D. Zheng, R. Na, S. Wang, and S. Zhang, "Eeg classification of motor imagery using a novel deep learning framework," *Sensors*, vol. 19, no. 3, p. 551, 2019.
[57] S. Kumar, A. Sharma, and T. Tsunoda, "An improved discriminative filter bank selection approach for motor imagery eeg signal classification using mutual information," *BMC bioinformatics*, vol. 18, pp. 125–137, 2017.
[58] R. Zhang, Q. Zong, L. Dou, and X. Zhao, "A novel hybrid deep learning scheme for four-class motor imagery classification," *Journal of neural engineering*, vol. 16, no. 6, p. 066004, 2019.